10.1109/ULTSYM.2011.0589

A Monte Carlo study on the effects of erythrocyte oxygenation on photoacoustic signals

Ratan K. Saha and Michael C. Kolios
Department of Physics, Ryerson University
350 Victoria Street, Toronto. M5B 2K3, Canada
Emails: ratank.saha@gmail.com, mkolios@ryerson.ca

***Abstract*—A theoretical model to study the effects of erythrocyte oxygenation on photoacoustic (PA) signals is described. An erythrocyte was considered as a fluid sphere and for such a sphere the PA field was computed by using a frequency domain approach. The linear superposition principle was used to obtain the resultant PA field generated by a collection of red blood cells (RBCs). A Monte Carlo algorithm was used to simulate 2D tissue realizations consisting of oxygenated RBCs (RBCOs) and deoxygenated RBCs (RBCDs). The oxygen saturation level of RBCOs was assumed to be 100% and 0% for RBCDs. The proportion of RBCOs and RBCDs fixed the oxygen saturation (SO_2) of a blood sample as, $SO_2 = N_O/(N_O + N_D)$, where N_O and N_D represent the numbers of RBCOs and RBCDs. The simulation results showed that the mean PA signal amplitude decreased monotonically as the SO_2 level increased for the 700 nm laser radiation. The same quantity exhibited a monotonic rise as the SO_2 level increased for the 1000 nm optical source. The PA amplitude demonstrated nearly 6 fold decrease and 5 fold increase, respectively at those wavelengths when SO_2 level varied from 0 to 100%. Spectral intensity in the low frequency range (< 10 MHz) also decreased for the first laser and increased for the second laser with increasing SO_2. However, these trends were not distinctly observed between 10-100 MHz. The simulated trends were in accordance with other experimental works. This suggests the suitability of this formulation to model the PA signal behaviors at different SO_2 levels.**

Keywords: Photoacoustics for RBCs, RBC oxygenation, Blood oxygen saturation, Monte Carlo simulation.

I. Introduction

Photoacoustic (PA) imaging technique is a hybrid modality [1]. In this technique, a short laser pulse irradiates a tissue medium, which absorbs light and under goes thermoelastic expansion. As a result of that, it emits a pressure pulse and that can be detected by a ultrasound transducer. The detected signal is useful to characterize as well as image the tissue medium. The contrast of a PA image is generally better than a conventional ultrasound backscatter image because the difference of optical absorption property is much more stronger than the impedance mismatch of different tissue regions. In PA, localized information can be obtained using a focused ultrasound transducer. Moreover, deeper tissue regions can be imaged using PA (compared to optical imaging modality) because it uses pressure waves, whose scattering is two to three orders of magnitude less than that of light and thus, travels longer distance.

The hemoglobin molecules that are present within the red blood cells (RBCs) behave as the dominant light absorbing chromophores and dictates the PA emission from RBCs. Recently, spatial maps of oxygenated RBCs (RBCOs) and deoxygenated RBCs (RBCDs) were generated for small animal brain imaging using PA technique [1]. This work exploited the large difference of absorption coefficients of RBCOs and RBCDs at some light wavelengths. Esenaliev et al., through *in vitro* experimental work showed that PA signal is very sensitive to the blood oxygen saturation (SO_2) for many incident optical radiations. The same group also demonstrated that it is feasible to measure blood SO_2 non-invasively by employing a PA technique.

This paper is about the modeling of PA signals from a collection of RBCs. For this purpose, we used a theoretical framework that was developed by our group [4]. The spatial organizations of non-overlapping randomly distributed mixtures of RBCOs and RBCDs in 2D were generated by employing a Monte Carlo algorithm. The oxygen saturation for RBCOs was assumed to be 100% and 0% for RBCDs. The proportion of RBCOs and RBCDs in such a mixture defined its SO_2 level. The PA signals were simulated from such samples. Both time domain and spectral domain features of the PA signals were examined as a function of blood SO_2.

II. Materials and methods

A. Theoretical model

The analytical expression of the PA field generated by a fluid sphere under the condition of thermal confinement can be written as [5],

$$p_f^{\text{single}}(r, k_f) = \frac{i\mu\beta I_0 v_s a^2}{C_P r} \times \frac{[\sin\hat{q} - \hat{q}\cos\hat{q}]e^{ik_f(r-a)}}{\hat{q}^2[(1-\hat{\rho})(\sin\hat{q}/\hat{q}) - \cos\hat{q} + i\hat{\rho}\hat{v}\sin\hat{q}]}. \quad (1)$$

The above solution can be obtained by solving the wave equation for the pressure field, originating due to the absorption of light, in the frequency domain and by matching the boundary conditions at the spherical boundary [5]. In (2), μ, C_P, β and a are the absorption coefficient, isobaric specific heat, thermal expansion coefficient and radius of the absorbing sphere, respectively. Further, $\hat{\rho} = \rho_s/\rho_f$ and $\hat{v} = v_s/v_f$ are the dimensionless density and speed of sound parameters, respectively. The subscripts s and f are used to indicate the spherical absorbing region and the surrounding fluid medium,

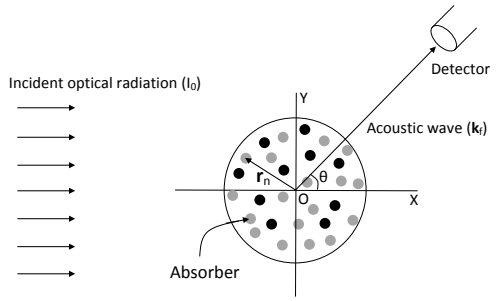

Fig. 1. Top view of the PA set up geometry. Black and grey filled circles represent two PA source populations with different absorption coefficients occupying the illuminated region. The PA signal is detected in the far field region.

respectively. The superscript single states that only one PA source is considered. Another dimensionless quantity $\hat{q}$ is defined as, $\hat{q} = \omega a/v_s = k_s a$. Here, k_s and k_f are the wave numbers of the acoustic wave within the absorbing region and the fluid medium, respectively. Moreover, ω is the modulation frequency of the incident optical radiation with intensity I_0.

If the illuminated region contains two populations of absorbing spheres with different optical absorption coefficients but otherwise with identical physical properties (e.g. mixtures of RBCOs and RBCDs), the generated PA field can be expressed in terms of linear superposition of waves that emitted by the individual cells as [4],

$$\begin{aligned} p_f^{\text{en}}(r,k_f) &\approx \frac{i\beta I_0 v_s a^2}{C_P r} \\ &\times \frac{[\sin\hat{q}-\hat{q}\cos\hat{q}]e^{ik_f(r-a)}}{\hat{q}^2[(1-\hat{\rho})(\sin\hat{q}/\hat{q})-\cos\hat{q}+i\hat{\rho}\hat{v}\sin\hat{q}]} \\ &\times \left[\mu_O\sum_{n=1}^{N_O} e^{-i\mathbf{k}_f\cdot\mathbf{r_n}} + \mu_D\sum_{n=N_O+1}^{N} e^{-i\mathbf{k}_f\cdot\mathbf{r_n}}\right]. \end{aligned} \quad (2)$$

Here, N_O is the number of RBCOs with absorption coefficient μ_O and $N_D = N - N_O$ is the number of RBCDs with absorption coefficient μ_D. The superscript en indicates an ensemble of absorbers. A schematic diagram is shown in Fig. 1 to illustrate the geometry of the PA set up. The time dependent PA field for uniform illumination by a delta function heating pulse can be obtained by using the Fourier transformation as,

$$\begin{aligned} p_f^{\text{en}}(r,t) &\approx \frac{i\beta F v_s a^2}{2\pi C_P r}\int_{-\infty}^{\infty} d\omega \\ &\times \frac{[\sin\hat{q}-\hat{q}\cos\hat{q}]e^{ik_f(r-a-v_f t)}}{\hat{q}^2[(1-\hat{\rho})(\sin\hat{q}/\hat{q})-\cos\hat{q}+i\hat{\rho}\hat{v}\sin\hat{q}]} \\ &\times \left[\mu_O\sum_{n=1}^{N_O} e^{-i\mathbf{k}_f\cdot\mathbf{r_n}} + \mu_D\sum_{n=N_O+1}^{N} e^{-i\mathbf{k}_f\cdot\mathbf{r_n}}\right], \end{aligned} \quad (3)$$

where F is the fluence of the optical radiation. In this work, (4) was evaluated to simulate PA signals from various samples.

B. Simulation method

A 2D region of interest (ROI) was considered in this work and that was uniformly irradiated by the optical radiation. Simulations in 2D are computationally less expensive than that of 3D but sufficient insight can be gained by examining 2D samples. The size of the ROI was taken as 200 μm $\times$ 200 μm. The ROI was composed of mixtures of RBCOs and RBCDs under non-overlapping conditions at hematocrit, $H = 45\%$. The fractional area occupied by the cells is defined as the hematocrit. The proportion, at which the RBCOs and RBCDs was mixed, fixed the oxygen saturation of a sample as, $SO_2 = N_O/(N_O + N_D)$. The cells were positioned within the ROI using a Monte Carlo algorithm known as the random sequential adsorption technique [6]. Fig. 2 displays simulated tissue realizations corresponding to 40% and 70% blood SO_2 levels.

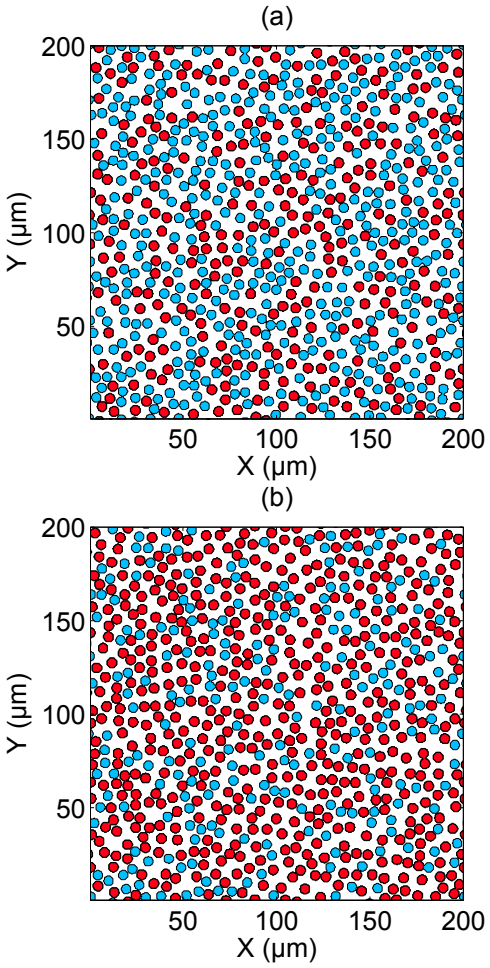

Fig. 2. (a) A simulated tissue realization consisting of spatially random distributions of RBCs for SO_2 = 40% at 45% hematocrit. Dark/red circles (40% of the total number of cells) represent RBCOs and grey/cyan circles (60% of the total number of cells) denote RBCDs. (b) Same as (a) but for SO_2 = 70% with $N_O : N_D = 7 : 3$.

The numerical values of the physical properties of an erythrocyte used in the simulations are presented in Table I [7]. The cells were suspended in a saline water and its physical

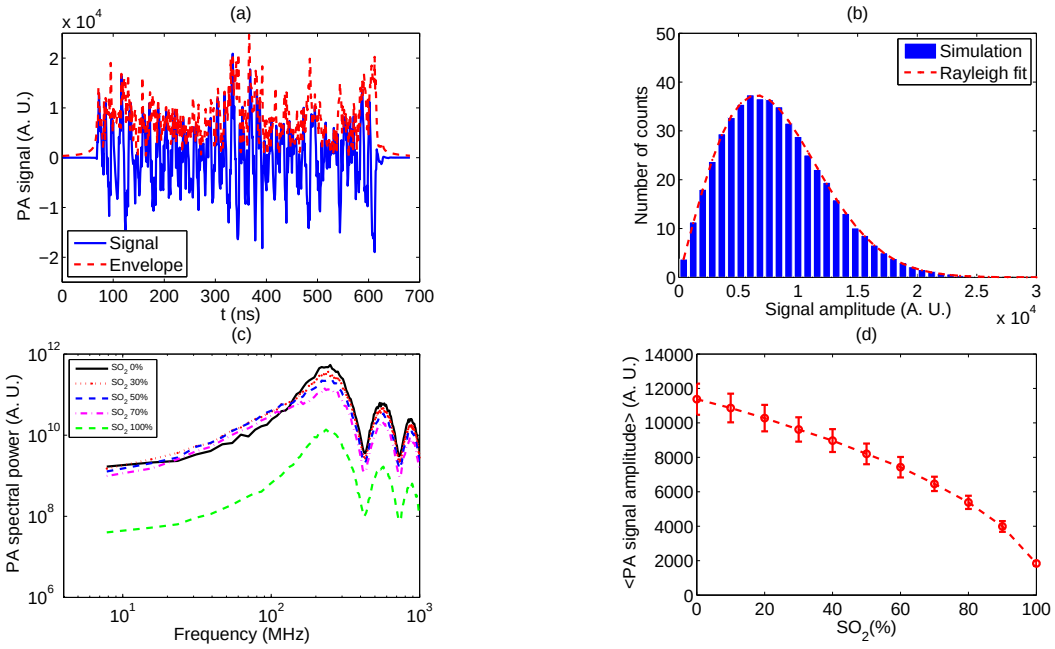

Fig. 3. (a) Plot of a simulated PA RF line along with its envelope for a mixture of RBCOs and RBCDs at $SO_2 = 50\%$, when illuminated by a 700 nm laser source. (b) Envelope histogram averaged over 250 lines and the best fit Rayleigh distribution curve. (c) Plots of power spectral lines for various SO_2 levels. (d) Variation of the mean PA amplitude ($\pm$ SD) as a function of SO_2.

properties are also given in Table I. The absorption coefficient of the medium inside a RBCO was estimated by multiplying the concentration of hemoglobin molecules inside the cell with the molar extinction coefficient for oxygenated hemoglobin molecules [8]. For this case, it was assumed that all the hemoglobin molecules were fully oxygenated. Note that an approximately 280 million hemoglobin molecules are present within a RBC having a volume of 87 μm^3 [9] and that provides a concentration of about 5.34×10^{-3} moles/l. Similarly, the absorption coefficient for a RBCD was estimated using the molar extinction coefficient for deoxygenated hemoglobin molecules [8]. The absorption coefficients were computed for the 700 and 1000 nm incident laser radiations and are displayed in Table II.

A computer code was written in C simulating time dependent PA field and was executed in a personal computer (OS: Windows 7, RAM: 4 GB and Processor: AMD Athlon (tm) II P320 Dual-Core, 2.10 GHz). It took about 3 min 44 seconds to generate 250 radio frequency (RF) lines. The post processing of simulated data was performed in MATLAB R2009b. The integral in (4) was numerically evaluated by implementing the trapezoidal rule for various samples. The computed pressure at each time point was a complex quantity. The real parts of the time series data provided the RF signal. The signal amplitude as a function of time was obtained from the absolute values of the complex time series data set. For each saturation level, 250 RF lines were generated from 250 tissue configurations. The signal envelope histogram averaged over 250 lines was obtained and fitted with a Rayleigh distribution curve. The best fit Rayleigh distribution curve was obtained by using a MATLAB optimization function.

TABLE I
NUMERICAL VALUES OF THE PHYSICAL PARAMETERS USED IN SIMULATIONS.

ROI	200 μm $\times$ 200 μm
H	45%
N	758
a	2.75 μm
ρ_s	1092 kg/m^3
v_s	1639 m/s
ρ_f	1005 kg/m^3
v_f	1498 m/s
β	1 K^{-1}
C_P	1 J kg^{-1}K^{-1}
F	1 Jm^{-2}

TABLE II
ABSORPTION COEFFICIENTS OF THE RBCOS AND RBCDS AT TWO INCIDENT LASER WAVELENGTHS.

Wavelength (nm)	μ_O (m^{-1})	μ_D (m^{-1})
700	356.64	2206.60
1000	1259.31	254.30

III. SIMULATION RESULTS

A simulated PA RF line is displayed in Fig. 3(a) for a sample with $SO_2 = 50\%$, when illuminated by a 700 nm laser source. The time variation of the signal amplitude is also shown in the same figure. Sharp variations of PA amplitude can be observed and that is because of the presence of very high frequency (e.g. GHz) components. The corresponding envelope histogram averaged over 250 RF lines and the best fit Rayleigh distribution curve are shown in Fig. 3(b). The Rayleigh distribution provided good fit to the histogram. The power spectral lines for various SO_2 levels are plotted in Fig.

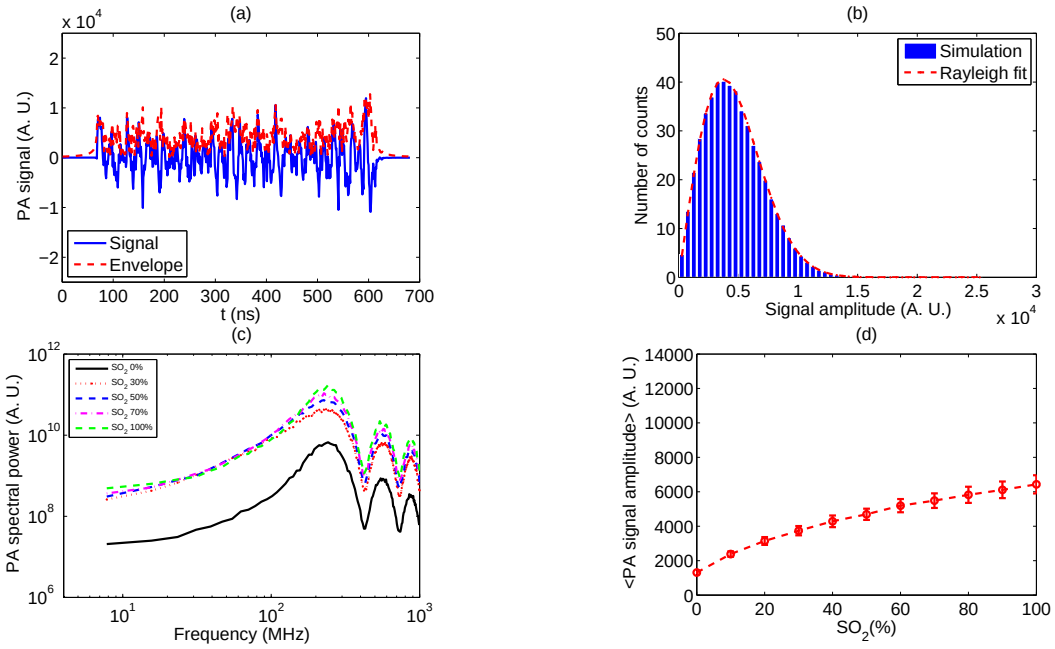

Fig. 4. Representative plots of a PA RF line and its envelope computed from a sample with $SO_2 = 50\%$, when irradiated by a 1000 nm optical radiation. (b) Envelope histogram averaged over 250 lines and the best fit Rayleigh distribution curve. (c) Plots of power spectral lines for various SO_2 levels. (d) Variation of the mean PA amplitude ($\pm$ SD) as a function of SO_2.

3(c) over a wide range of frequencies (MHz to GHz). The spectral power decreased as the SO_2 increased. This trend is distinctively clear up to 10 MHz, but after that they overlap for some cases. The spectral power at $SO_2 = 0\%$ at each frequency is almost 36 times more than that of $SO_2 = 100\%$, since in this case, $\mu_O : \mu_D \approx 1 : 6$. Fig. 3(d) illustrates how mean PA signal amplitude ($\pm$ SD) varies with SO_2. It exhibits a monotonic decrease with SO_2 and an approximately 6 fold decrease can be noted.

Fig. 4(a) shows a PA RF line at $SO_2 = 50\%$ for a 1000 nm light source. Associated envelope histogram is displayed in Fig. 4(b). The Rayleigh distribution also provided good fit to the histogram. The power spectral lines are plotted in Fig. 4(c) for a series of SO_2 levels. As the SO_2 increased, spectral power also increased. Fig. 4(d) demonstrates the variation of mean PA signal amplitude with SO_2. The PA amplitude increased about 5 times at $SO_2 = 100\%$ than that of $SO_2 = 0\%$ since in this case, $\mu_O : \mu_D \approx 5 : 1$.

IV. Discussion and Conclusion

A theoretical model is presented to examine the effects of blood SO_2 on PA signals. For this purpose, mixtures of RBCOs and RBCDs were considered. The resultant signal from an ensemble of RBCs was computed by using the linear superposition principle for signals emitted by individual RBCs. It was observed that PA signal amplitude increased as the SO_2 decreased for the 700 nm optical radiation. However, for the 1000 nm incident light beam, PA signal amplitude increased with increasing SO_2. These trends are in agreement with published experimental results. For example, Esenaliev et al. [2], found a linear trend with SO_2 in an *in vitro* experimental work for a 1064 nm laser source. The same group in an *in vivo* experimental work obtained monotonic decrease with SO_2 for the 700 nm source [3]. Nevertheless, they measured linear increase with SO_2 for the 1064 nm source. The general agreement between simulation and experimental results suggests the suitability of this theoretical framework to model the PA signal behaviors at different SO_2 levels.

Acknowledgment

We would like to gratefully thank the funding agencies (Canadian Institutes of Health Research (CIHR) grant MOP-97959, CIHR grant from the Terry Fox Foundation and the Canada Research Chairs Program awarded to M. C. Kolios) for supporting this work. We also thank Dr. M Rui, Dr. S Narshimhan and Mr. E Hysi for their interests and encouragements during this work.

References

[1] L. V. Wang, Med. Phys., 35(12), 5758-5767, 2008.
[2] R. O. Esenaliev *et al.*, Applied Optics, 41(22), 4722-4731, 2002.
[3] H. P. Brecht *et al.*, Optics Express, 15(24), 16261-16269, 2007.
[4] R. K. Saha and M. C. Kolios, J. Acoust. Soc. Am., 129(5), 2935-2943, 2011.
[5] G. J. Diebold, "Photoacoustic monopole radiation: Waves from objects with symmetry in one, two and three dimensions", Photoacoustic imaging and spectroscopy, Edt. L. V. Wang, Taylor and Francis Group, LLC, 2009, Chapter 1, pp. 3-17.
[6] E. L. Hinrichsen, J. Feder and T. Jøssang, Phys. Rev. A, 41, 4199-4209, 1990.
[7] K. K. Shung, Y. W. Yuan, D. Y. Fei and J. M. Tarbell, J. Acoust. Soc. Am., 75, 1265-1272, 1984.
[8] Data complied by S. Prahl at http://omlc.ogi.edu/spectra.
[9] S. I. Fox, "Human Physiology", McGraw-Hill, New York, 2008, Tenth Edition, Chapter 13, pp. 388-430.